

# A NEW APPROACH FOR MEMS POWER GENERATION BASED ON THERMOACOUSTIC HEAT ENGINE

M. Serry<sup>1,2</sup>, A. Abdel Aziz<sup>2</sup>, E. Abdel Rahman<sup>2</sup> and S. Sedky<sup>2</sup>

<sup>1</sup>King Abdullah University of Science and Technology, Thuwal, Saudi Arabia

<sup>2</sup>Yousef Jameel Science and Technology Research Center, The American University in Cairo, Egypt

**Abstract:** A new approach of a MEMS power generator based on a Thermoacoustic Heat Engine (TAHE) that converts waste heat into electrical power is presented. A MEMS-TAHE design is introduced taking into account material limitations and process flow for a high temperature gradient micro-stack structure. Moreover, energy and heat transfer simulations for the micro-stack structure demonstrate the functionality of the engine in the microwatts power range. This work presents the theoretical and practical implications of miniaturizing thermoacoustic power generators. In addition, the design and material challenges of different micro-stack geometries are summarized and compared.

**Keywords:** Thermoacoustics, Heat Engine, MEMS, Miniaturization

## INTRODUCTION

### Principle of Power Generation

Thermoacoustic heat engines (TAHE) are simple devices that efficiently convert heat to intense acoustic power through the positive feedback loop between heat transfer and acoustic energy [1,2]. They work without any solid moving parts and exhibits self-excited oscillations when a temperature difference is maintained across the stack, Fig. 1. TAHE can be utilized to generate electricity [3] by generating and maintaining a temperature difference between a hot heat exchanger and cold heat exchanger along the stack of parallel plates. The generated acoustic energy can be transformed to an electrical energy through an array of piezoelectric transducers. Fabrication of MEMS-TAHE power generator is very challenging yet favorable because of its high power density. The proposed approach introduces non-moving-parts, high power density, combustion-free, long-life and environmentally friendly micropower generation device that contributes to the recent development in the field of microscale heat engines.

### Miniaturization Challenges

Current efforts toward the miniaturization of TAHE devices were faced by many physical and technological challenges. Major challenges are the high onset temperature (typically 1500°C/cm), the large temperature difference that should be maintained across a microscale stack, and the thermal and viscous losses due to boundary effects [4].

Accordingly, in this paper, a new design approach for MEMS Thermoacoustic Heat Engine based on maximizing the efficiency of power conversion through initiating and maintaining large temperature difference across the micro-stack is

proposed.

The paper also discusses the ongoing challenges for implementation, including integrated diamond like carbon material to enhance the performance of the heat sink, microscale thermal isolation, piezoelectric membrane integration, large aspect ratio micro-features, and suggestions to increase the efficiency of power conversion.

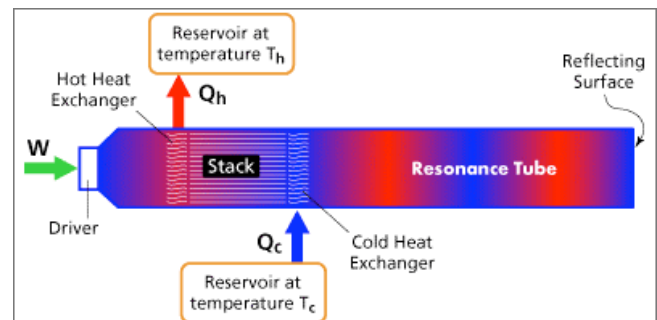


Fig. 1: Principle and components of a thermoacoustic heat engine/refrigerator.

## DESIGN AND FABRICATION OF MEMS THERMOACOUSTIC HEAT ENGINE

Building on the existing efforts towards the thermoacoustic heat Engine's miniaturization we propose the design shown in Fig. 2 of the first full MEMS scale TAHE. Our design approach is to maximize the efficiency of power conversion through initiating and maintaining large temperature difference across the micro-stack.

By utilizing materials available for MEMS technology the design's functionality together with the fabrication feasibility was achieved as follows:

- The stack's pillars are formed of SiO<sub>2</sub> to decrease heat conduction along the stack.

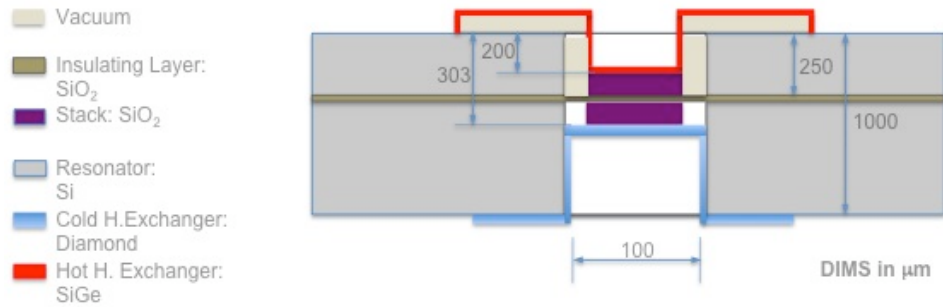


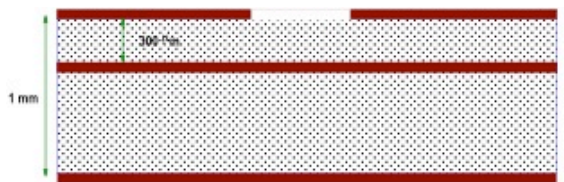
Fig. 2: A schematic showing the design and materials of the proposed MEMS thermoacoustic heat engine.

- A SiGe layer with large surface area is deposited at the hot part to increase the input heat flux.
- A vacuum gap is formed at the sides of the stack to eliminate the transverse heat conduction with the silicon substrate.
- SOI wafer with thick buried oxide is used initially to minimize heat conduction across the hot and cold sections.

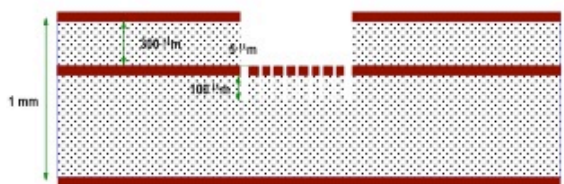
- A diamond-like-carbon layer is deposited to increase heat conduction at the cold end of the engine and help maintain the large temperature difference across the stack.

Accordingly, a fabrication process flow for a quarter wavelength thermoacoustic engine is summarized as follows (see Fig. 3):

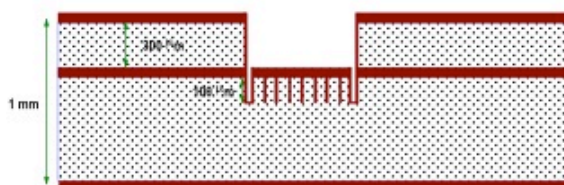
- Starting with SOI wafer with a 4 μm thick top, bottom and buried oxide.



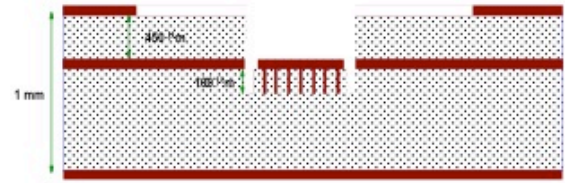
a) Starting from SOI wafer, Etch the top oxide



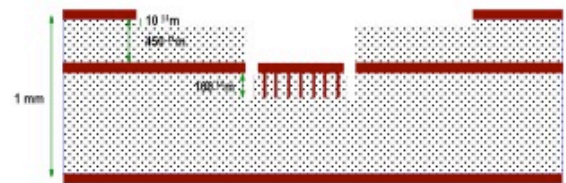
b) Etch and Pattern the buried oxide, then etch 100 μm deep trench in Si



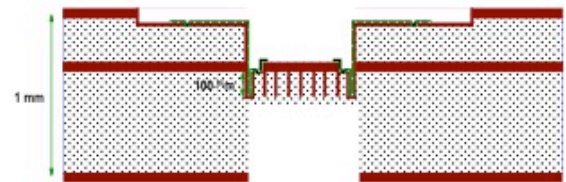
c) Deposit 2 μm SiO<sub>2</sub>.



d) Etch 4 μm top SiO<sub>2</sub> layer.



e) Etch 10 μm trench in Si



f) Deposit and pattern 1 μm SiGe then Etch the backside of Si

Fig. 3 (Continued): Summary of the process flow

- Pattern the top oxide to form the resonator's top part.
- Pattern and etch the pillars of the micro-stack.
- Deposit 2 μm SiO<sub>2</sub> layer to form the pillars of the micro-stack.
- Pattern the top oxide part and then deposit the SiGe layer that will function as the hot part of the stack.
- Repeat the patterning and etching a bottom side to form the complete resonator.
- Deposit the diamond-like-carbon (DLC) layer at the bottom part of the resonator to function as the cold part of the stack.
- Finally, release of the SiGe top layer and generation of vacuum to prevent heat conduction between the SiGe hot part and the Si substrate.

Fig. 3: Summary of the process flow

## FINITE ELEMENT SIMULATIONS

Transient heat transfer analysis was performed on the proposed micro-stack using ANSYS. The simulations showed that a temperature difference of 80°C can be successfully maintained across the micro-stack with an input heat flux of 10000 W/m<sup>2</sup> (through a sun concentrator). A vacuum boundary condition at the stack's periphery, and infinite heat sink boundary conditions at the diamond bottom part were assumed.

Fig. 4 shows temperature gradient across the stack at steady state (after 4 seconds of initialization).

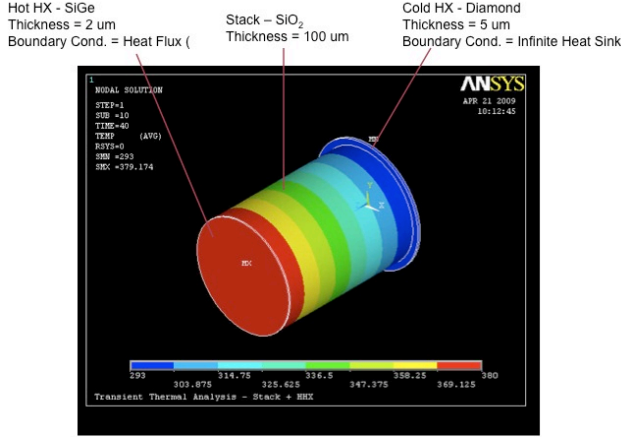


Fig. 4: F.E. simulations of the temperature gradient across the micro-stack

It is worth noting that heat losses due to the working fluid flow and possible leakages were not taken into account in the F.E. simulations. However they're expected to be of the minimal effect on the generated temperature gradient.

## THEORETICAL ANALYSIS

According to linear thermoacoustics [5-7] the ratio of the temperature gradient along the stack normalized to the critical temperature gradient is given by:

$$\Gamma = \nabla T_m / \nabla T_{crit} \quad (1)$$

for the heat engine to deliver power, the mean temperature gradient along the stack must be larger than the critical temperature gradient:

$$\nabla T_m > \nabla T_{crit} \quad (2)$$

theoretically, the critical temperature gradient,  $\nabla T_{crit}$  is proportional to the frequency of the heat engine and depends on geometrical factors and the calculated

critical temperature gradient in a standing wave depends on the wavelength and the stack location,  $x$ , from the nearest pressure anti-node, as follows:

$$\nabla T_{crit} \cong \frac{T_m}{\lambda} \tan\left(\frac{x}{\lambda}\right), \quad (3)$$

where,  $\lambda$  is the sound wavelength normalized by  $2\pi$ .

And finally, the efficiency of the heat engine can be written in comparison to the carnot's efficiency can be expressed as follows:

$$\eta = \frac{\eta_c}{\Gamma}, \quad (4)$$

Using Eqns. 1 to 4 the critical temperature gradient, the maximum stack length and the overall efficiency can be calculated as a function in the normalized stack length,  $\frac{x}{l}$ . Table 1 summarizes the effects of normalized stack length on the overall efficiency at a temperature difference across the stack of 80°C and a 1mm resonator's length.

Table 1: Calculation of the overall efficiency as a function in the normalized stack location.

Normalized Stack Location $\left(\frac{x}{l}\right)$	Critical Temperature Gradient ( $\nabla T_{crit}$ ) (°K/μm)	Overall Efficiency ( $\eta$ )
0.85	0.13	1%
0.5	0.52	4%
0.4	0.72	6%
0.3	1	8%
0.2	1.6	13%
0.1	3.3	27%

## DISCUSSION

The main objectives of our study are to maintain high temperature difference along the stack length and to maximize the overall efficiency of the MEMS TAHE device. While the first objective was successfully achieved through the proposed design and material selection as demonstrated by the F.E. simulations, the second objective can be mainly controlled through the proper selection of the stack's location and the resonator's length.

Stack's location affects two important parameters, 1) the power output of the device: it should optimally be placed at the location of the maximum sound wave

momentum (i.e., at  $x/l=0.5$  for a quarter wave length), and 2) the critical temperature gradient and the overall efficiency as demonstrated in Eqns. 3 and 4 and Table 1.

Accordingly, a trade off in the power output and the overall efficiency is normally expected and it optimized according to the application. For the case of MEMS-TAHE, a great number of devices can be produced per each wafer which results in an increased power output and power density.

Therefore, the overall efficiency of the device along with feasibility and easiness of fabrication are the major factors in the case of MEMS-TAHE. According to Table 1 and Figs 5 and 6, these two factors can be satisfied at a normalized stack location,  $x/l$  of 0.1 at which the overall theoretical efficiency can reach up to 27% per device.

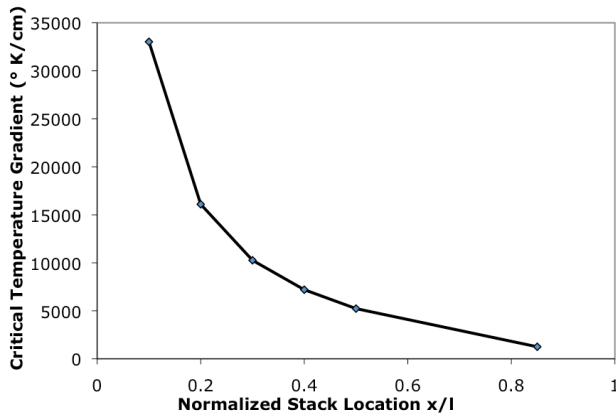


Fig.5: Effect of stack location on the critical temperature gradient

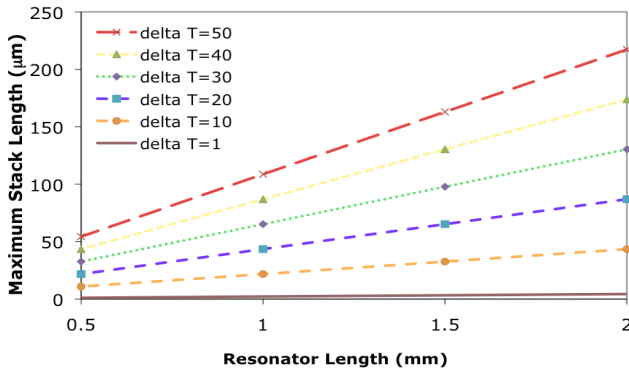


Fig. 6: Effect of resonator's length on the maximum stack length at different temperature differences

## CONCLUSIONS

The paper proposed a new design approach for MEMS Thermoacoustic Heat Engine based on maximizing the efficiency of power conversion through initiating and maintaining large temperature difference across the micro-stack as follows. 1) The stack's pillars are formed of  $\text{SiO}_2$  to decrease heat conduction along the stack. 2) A SiGe layer with large surface area is deposited at the hot part to increase the input heat flux. 3) A vacuum gap is formed at the sides of the stack to eliminate the transverse heat conduction with the silicon substrate. 4) SOI wafer with thick buried oxide is used initially to minimize heat conduction across the hot and cold sections. 5) A diamond-like-carbon layer is deposited to increase heat conduction at the cold end of the engine and help maintain the large temperature difference across the stack.

Finite element simulations and theoretical analysis of different design configurations showed that a temperature difference of  $80^{\circ}\text{C}$  is successfully maintained across the stack leading to a theoretical power conversion efficiency of 27%.

The paper also discussed the ongoing challenges for implementation, and suggestions to increase the efficiency of power conversion.

## REFERENCES

- [1] G.W. Swift, Thermoacoustic engines, Journal of Acoustical Society of America 84 (1988) 1145
- [2] S. Backhaus, G.W. Swift, A thermoacoustic stirling heat engine, Nature 399 (1999) 335–338
- [3] O.G. Symko, E. Abdel-Rahman, Y.S. Kwon, M. Emmi, R. Behunin. Design and development of high-frequency thermoacoustic engines for thermal management in microelectronics, Microelectronics Journal, 35, (2004) 185–191
- [4] C. Tsai, R. Chen, C. Chen, J. DeNatale, Micromachined Stack Component for Miniature Thermoacoustic Refrigerator, MEMS 2002, Fifteenth IEEE International Conference on Micro Electro Mechanical Systems, Piscataway, NJ (2002) p. 149
- [5] N. Rott, Thermoacoustics, Advances in Applied Mechanics 20 (1980) 135
- [6] G. W.Swift, Thermoacoustic engines and refrigerators, Physics Today July (1995) 22
- [7] S. Garrett, T. Hofler, Thermoacoustic Refrigeration, Technology 2001. NASA Conference Publication 3136 (1991) 397